Bit and Power Loading Algorithms for Nonlinear Optical Wireless Communication Channels

Jakub Kasjanowicz, Juliusz Bojarczuk, Grzegorz Stepniak

Abstract—Bit and power loading (BPL) algorithms played a pivotal role in the success of orthogonal frequency division multiplexing (OFDM) in digital transmission, including light-emitting diode (LED) based wireless optical communications. Nevertheless, the conventional BPL algorithms do not distinguish the nonlinear distortion generated in LED transmitters from an additive noise, which leaves room for improvement. This letter presents a novel power loading and two BPL algorithms that maximize the transmission capacity while minimizing the nonlinear distortion generated in LED. The effectiveness of the proposed algorithms is evaluated through simulations and transmission experiments, revealing a throughput increase of up to 10% in comparison to what can be achieved employing classical algorithms.

Index Terms—OWC, nonlinear, OFDM, bit and power loading algorithm, Light-emitting diodes.

I. INTRODUCTION

AS the demand for high-speed data transmission continues to grow with the advancement and proliferation of wireless devices, traditional RF-based communication systems are besieged with challenges of spectrum scarcity and interference. In light of these limitations, optical wireless communications (OWC) has emerged as a promising alternative [1]. Visible light communications (VLC) utilizes light-emitting diodes (LEDs) for illumination and "wireless" data transmission, providing a blend of functionality and communication capabilities. VLC has numerous advantages: it utilizes the unregulated and abundant visible light spectrum, avoids contributing to radio frequency congestion, and offers enhanced security as light signals are confined to specific areas, making it difficult for eavesdroppers to intercept the communication unless they are physically within the vicinity of the light source [2].

To maximally utilize the available modulation bandwidth of the LED, VLC systems often employ advanced modulation formats, like orthogonal frequency division multiplexing (OFDM) [3], [4]. Among several advantages, OFDM, as a multicarrier scheme, is capable of optimizing the number of bits being transmitted and powers in different subcarriers to maximize the transmission capacity. As an example, in a low-pass LED channel, more bits are allocated in subcarriers at lower frequencies, where the channel attenuation is lower [4]. However, the optimal allocation of bits and powers to the subcarriers poses a constrained multivariable mixed-integer nonlinear optimization problem. The only exact solution known as "water-filling" (WF) can be reached using Lagrangian optimization, but only when the problem is relaxed to power allocation [4], [5]. In practical communication systems, a suboptimal bit and power distribution is methodically achieved by the application of discrete bit- and power-loading algorithms (BPL). These greedy-type iterative procedures first send a uniformly loaded testing signal to estimate the signal-to-interference-plus-noise ratio (SINR) distribution in the subcarriers. Subsequently, an offline BPL algorithm assigns the number of bits and power to each subcarrier based on the SINR. There are two main classes of BPL algorithms: one that targets rate maximization (e.g., Hughes-Hartogs (HH) [6]) and one that targets margin maximization (e.g., Levin-Campello (LC) [7]) under the constraint of total power and bit rate, respectively.

A comprehensive study of BPL in VLC is provided in [4], where the authors consider the following power loading strategies specifically for LED channels: water-filling, uniform, and preemphasis. In preemphasis, a filter with an inverse response to the channel is applied at the transmitter, so the overall system gain in the frequency domain is flat, and bits are loaded uniformly. It is concluded that uniform power loading is 1-2 % short in capacity compared with water-filling, while the preemphasis approach has a considerable penalty with respect to the two. Although the analysis in [4] considered static LED nonlinearity to find the optimum bias current, the whole investigation of BPL was performed under a linear LED channel assumption. Unfortunately, LED is a nonlinear device with well-documented dynamic nonlinear behavior. In addition, OFDM signal has a high peak-to-average power ratio (PAPR) and is known to be susceptible to nonlinear distortion (ND) of LED transmitters [8]. Only one paper aimed at proposing a power-only allocation algorithm that takes into account the nonlinear LED response [9]. In other areas of digital transmission, the literature on the topic is also limited. In a wireless system with a nonlinear power amplifier, BPL with a conventional HH algorithm was proposed, but only to the point when further allocation will not lead to capacity improvement due to the buildup of ND [10]. In [11], a power-only allocation scheme based on particle swarm optimization is proposed. The scarcity of literature is most probably due

Jakub Kasjanowicz, Juliusz Bojarczuk, and Grzegorz Stepniak are with the Institute of Telecommunications, Warsaw University of Technology, 00-665 Warsaw, Poland (e-mail: jakub.kasjanowicz.stud@pw.edu.pl; juliusz.bojarczuk@pw.edu.pl; grzegorz.stepniak@pw.edu.pl).

to the fact that without a reliable model of the channel nonlinearity, the BPL algorithm cannot work as described, i.e., with single channel estimation and offline optimization, but would require retransmission each time an additional bit is loaded to estimate ND generated. In [9], this problem is circumvented by replacing retransmissions with resimulations in a previously estimated Volterra representation of the LED and applying particle swarm optimization like in [11].

There are three main contributions of this letter. First, we propose to tackle the nonlinear distortion by using BPL algorithms and study the theoretical efficiency of such an approach. Second, we propose three practical algorithms that implement the idea. Third, we achieve a 10% data rate increase for LED transmission in a nonlinear regime. The BPL algorithms apply the block-based LED model proposed in our previous papers [12], [13] to predict the impact of an extra bit allocated on the ND distribution over OFDM subcarriers. Our analysis is restricted to the 2nd order of ND, as this order dominates at practical LED driving input powers [13], [14].

II. THEORY

We consider an OFDM line-of-sight LED transmission system with a total of N subcarriers, number of bits at ith subcarrier $B(i)$, and power of the subcarrier $P(i)$. We identify two input power regimes: a linear one and a nonlinear one. In the linear one, the input signal power equals $P_{tot}^{(1)} = \sum P(i)$ and is too small to generate ND at a level sufficient to degrade the transmission performance, hence the SINR at the receiver equals [4]

$$\sigma^{(1)}(i) = \frac{P(i)G^2(i)}{N_0},\qquad(1)$$

where $G(i)$ is the amplitude response of the LED at the ith subcarrier and N_0 is the additive white receiver noise power across all subcarriers. At the target input power, which falls in the nonlinear regime, the input power is M times higher than in the linear and equals $P_{tot}^{(M)} = \sum P(i) = P_{tot}^{(1)} \cdot M$, where $M > 1$. In the nonlinear regime, the nonlinear distortion adds to the noise term, and SINR equals

$$\sigma^{(M)}(i) = \frac{P(i)G^2(i)}{N_0 + \mathrm{ND2}(i)},\qquad(2)$$

where $\mathrm{ND2}(i)$ is the 2nd order ND power at subcarrier i. Specifically, [12]

$$\mathrm{ND2}(i) = \frac{1}{4}\sum_k |G_2(k, i-k)X(k)X(i-k)|^2,\qquad(3)$$

where $X(i)$ is the complex envelope of the ith subcarrier signal, $G_2(i, j)$ is the 2nd order Volterra kernel of LED in the frequency domain [13]. The two regimes can be identified by observing that in the linear regime, SINR distribution at the receiver increases proportionally to the input power and follows the channel frequency response (see: Fig. 2(e)). In the nonlinear regime, the rate of increase of SINR is reduced, or it may even decrease with an increase in input power.

A nonlinearity-aware BPL algorithm must know the ND distribution dependence on the input signal. Unfortunately, the ND at a given subcarrier depends on the powers of all

the subcarriers (3), and evaluation of (3) requires cumbersome estimation of the Volterra frequency domain kernel [14], [15]. Instead, we propose to apply the following heuristic: (i) ND power depends on a constant γ and on the square of the signal power at the input to the nonlinear element in the system; (ii) ND spectral distribution $S(i)$ is identical to the distribution under uniform power loading. The assumption (i) stems from the property of 2nd-order nonlinear systems in general, in which the power of the 2nd-order ND product is proportional to the square of the input power[1], while γ is a coefficient, which captures the nonlinear properties of the LED at a given bias current, temperature, etc. This formulation requires some LED model to determine the power of the signal at nonlinearity input. In [12], [13], we have shown that the 2nd order Volterra kernel of LED can be decomposed into 3 consecutive blocks: linear filter equal to the LED frequency response $G(i)$, squaring $()^2$ and filtering with $H_2(i)$ (Fig. 1(a)). Consequently, the power at the input to nonlinearity (i.e., squaring) is $\sum_i P(i)G^2(i)$. Finally, assumption (ii) is motivated by the fact that even with the application of BPL algorithms, the power in the subcarriers rarely varies by more than 3 dB (see [5, Fig. 7], [4, Fig. 9]), as this is the typical power increment required to achieve a specific bit error rate (BER) for an additional bit in quadrature amplitude modulation (QAM). The frequency domain convolution in (3) further blends the power variation impact on the spectral distribution of ND. Thus, we assume the following equation for ND:

$$\mathrm{ND2}(i) = \gamma S(i)\left(\sum_i P(i)G^2(i)\right)^2,\qquad(4)$$

where $S(i)$ is normalized to its maximum. $S(i)$ and γ are estimated with uniform power loading at low ($P(i) = 1$) and high ($P(i) = M$) input powers from (5), where (5) is derived by equating (1), (2) and (4)

$$\gamma S(i) = \left(\frac{M}{\sigma^{(M)}(i)} - \frac{1}{\sigma^{(1)}(i)}\right)\frac{G^2(i)(M^2 - 1)^{-1}}{(\sum G^2(i))}.\qquad(5)$$

A. Nonlinear BPL algorithms

Before presenting nonlinear BPL algorithms, we introduce a power-only loading algorithm (Algorithm 1), which demonstrates the principle of ND-aware allocation. The algorithm initiates with all subcarriers turned off. Next, in each step, it adds a power increment Δ to a subcarrier for which the total Shannon's capacity (summed over all the subcarriers) is predicted the highest and terminates at the point when the power so far assigned $\sum P_c$ exceeds the total power available P_{lim}. As the formula for the capacity $C(n)$ includes the ND, the algorithm avoids loading power to subcarriers with a higher contribution to the ND.

The nonlinear BPL1 algorithm (Algorithm 2) applies the principle of (Algorithm 1) to bit loading: it calculates the SINR for every subcarrier upon loading an additional bit (and

[1] In 2nd order system given with equation $y = \alpha x + \beta x^2$, the power of the quadratic term depends on the quadruple of the amplitude and square of the input signal power.
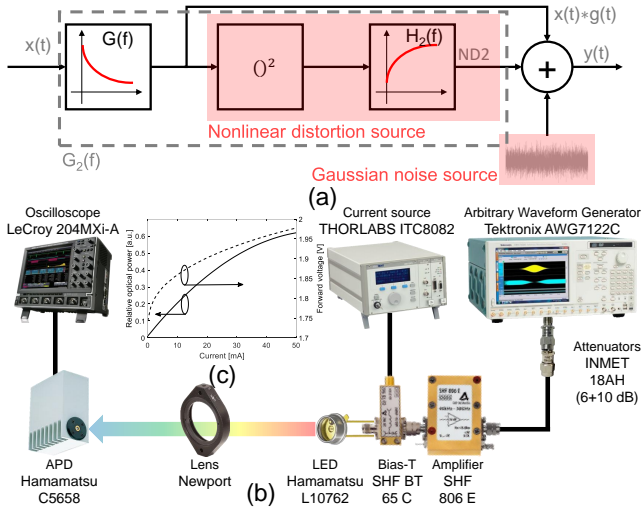
Fig. 1. (a) OWC channel model assumed in the nonlinear algorithms. (b) experimental setup. The distance between the APD and the LED is equal to 28 cm. (c) Light-current-voltage curve of utilized RC LED.

Algorithm 1 Power loading algorithm

$$max_{P_c(m)} \sum C(m) \quad s.t. \quad \sum P_c(m) < P_{lim}$$

1: $P_c(n) \leftarrow 0, n \in 1:N$
2: **while** $\sum P_c \leq P_{lim}$ **do**
3:     **for** $n \in 1:N$ **do**
4:         $P_{proj} \leftarrow P_c$
5:         $P_{proj}(n) \leftarrow P_{proj}(n) + \Delta$
6:         $\text{ND2}(n) \leftarrow \gamma S(n)(\sum_i P_{proj}(i)G^2(i))^2$
7:         $C(n) = \sum_m log_2\left(1 + \frac{P_{proj}(m)G^2(m)}{N_0 + \text{ND2}(m)}\right)$
8:     **end for**
9:     $m \leftarrow \max_m C(m)$
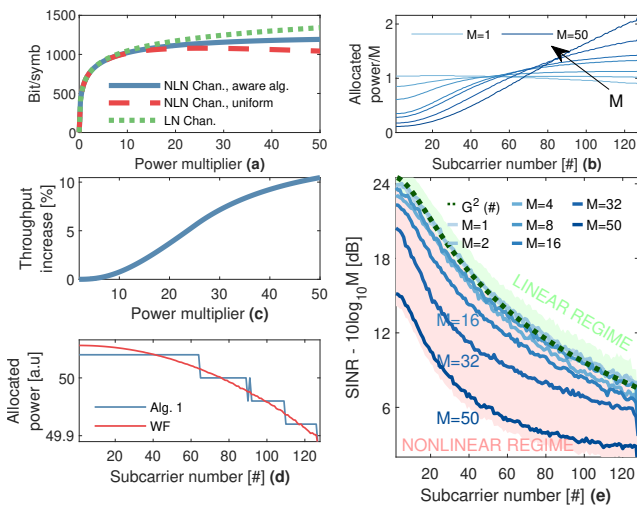10: $P_c(m) \leftarrow P_c(m) + \Delta$
11: **end while**

Fig. 2. (a) channel capacity for a linear channel (dotted line), a nonlinear channel with uniform power allocation (dashed line), a nonlinear channel with proposed nonlinearity-aware algorithm (solid line). (b) Optimal power distribution for various power multipliers. (c) Throughput increase after using a nonlinear algorithm (compared to water-filling). (d) Comparison of power allocation done by water-filling and Algorithm 1 in linear LED (i.e., $\gamma = 0$). (e) Estimated SINR for each subcarrier relative to the input signal power. Simulation parameters are given in Section III.

Algorithm 2 Nonlinear BPL1

$$max_{(P_c(m),B(m))} \sum B(m) \quad s.t. \quad \sum P_c(m) < P_{lim}$$

Require: $\sigma_r = SINR_{QAM}(P_e = BER_0)$
1: $P_c(n) \leftarrow 0, B(n) \leftarrow 0, n \in 1:N$
2: **while** $\sum P_c \leq P_{lim}$ **do**
3:     **for** $n \in 1:N$ **do**
4:         $P_{proj} \leftarrow P_c$
5:         $P_{proj}(n) \leftarrow \text{CALCPOWER}(n, B, P_c, 1)$
6:         $\text{ND2}(n) \leftarrow \gamma S(n)(\sum_i P_{proj}(i)G^2(i))^2$
7:         $C_r(n) = \sum_m log_2\left(1 + \frac{(P_{lim} - \sum_m P_{proj}(m))G^2(m)}{N(N0 + \text{ND2}(m))}\right)$
8:     **end for**
9:     $m \leftarrow \max_m C_r(m)$
10:     $B(m) \leftarrow B(m) + 1$
11:     $P_c(m) \leftarrow \text{CALCPOWER}(m, B, P_c, 0)$
12:     **for** $n \in 1:N$ **do**
13:         **if** $B(n) > 0$ **then**
14:             $P_c(n) \leftarrow \text{CALCPOWER}(n, B, P_c, 0)$
15:         **end if**
16:     **end for**
17: **end while**
18: **procedure** CALCPOWER(n, B, P, b) ▷ **Require:** $\sigma_r, N_0, S, G, \gamma$
19:     **return** $\frac{\sigma_r(B(n)+b)(N_0 + \gamma S(n)\sum(P(i)G^2(i)))^2}{G^2(n)}$
20: **end procedure**

---

power), and subsequently selects to load the subcarrier for which the remaining capacity to be allocated with the remaining power is the highest. The power of this subcarrier is then increased to meet the required SINR at a target BER defined in table σ_r [7]. Finally, the power of every subcarrier is increased in order to account for the newly introduced ND that arose in the preceding stage. The nonlinear BPL2 algorithm presented in (Algorithm 3) is a modification of the HH algorithm [6]. However, unlike the original algorithm, which selects to load the subcarrier with the lowest power increment required, the proposed algorithm takes into consideration that an increase in the power of a specific subcarrier will necessitate a power adjustment in the remaining subcarriers due to the additional ND. The algorithm assigns the bit to the subcarrier with the lowest sum of power increments across all subcarriers and subsequently adjusts the power of the remaining subcarriers to accommodate the ND. It is important to note that since ND is a secondary order effect, we ignore any additional ND created by the mentioned adjustment. Finally, we remark upon the algorithm loop nesting that the HH and LC algorithms have linear complexity, while the complexity of BPL1 and BPL2 is quadratic and cubic, respectively. However, both BPL1 and BPL2 only need to be run once at system initialization, so their overall computational overhead is still relatively low.

III. NUMERICAL RESULTS

First, we investigate the performance of the nonlinear-aware power-only loading algorithm (Algorithm 1). We note that the resulting power distribution of Algorithm 1 in a linear LED (M=1, ND2=0) closely approximates the WF solution

---

Algorithm 3 Nonlinear BPL2

$$max_{(P_c(m),B(m))} \sum B(m) \quad s.t. \quad \sum P_c(m) < P_{lim}$$

Require: $\sigma_r = SINR_{QAM}(P_e = BER_0)$

1:   $P_c(n) \leftarrow 0, B(n) \leftarrow 0, n \in 1:N$
2:   **while** $\sum P_c \leq P_{lim}$ **do**
3:      **for** $n \in 1:N$ **do**
4:         $P_{proj} \leftarrow P_c$
5:         $P_{proj}(n) \leftarrow$ CALCPOWER$(n, B, P_c, 1)$
6:         **for** $m \in 1:N$ **do**
7:            **if** $m \neq n \wedge B(m) > 0$ **then**
8:               $P_{proj}(m) \leftarrow$ CALCPOWER$(m, B, P_c, 0)$
9:            **end if**
10:        **end for**
11:        $P_s(n) = \sum P_{proj}$
12:      **end for**
13:      $m \leftarrow \min_m P_s(m)$
14:      $B(m) \leftarrow B(m) + 1$
15:      $P_c(m) \leftarrow$ CALCPOWER$(m, B, P_c, 0)$
16:      **for** $n \in 1:N$ **do**
17:         **if** $B(n) > 0$ **then**
18:            $P_c(n) \leftarrow$ CALCPOWER$(n, B, P_c, 0)$
19:         **end if**
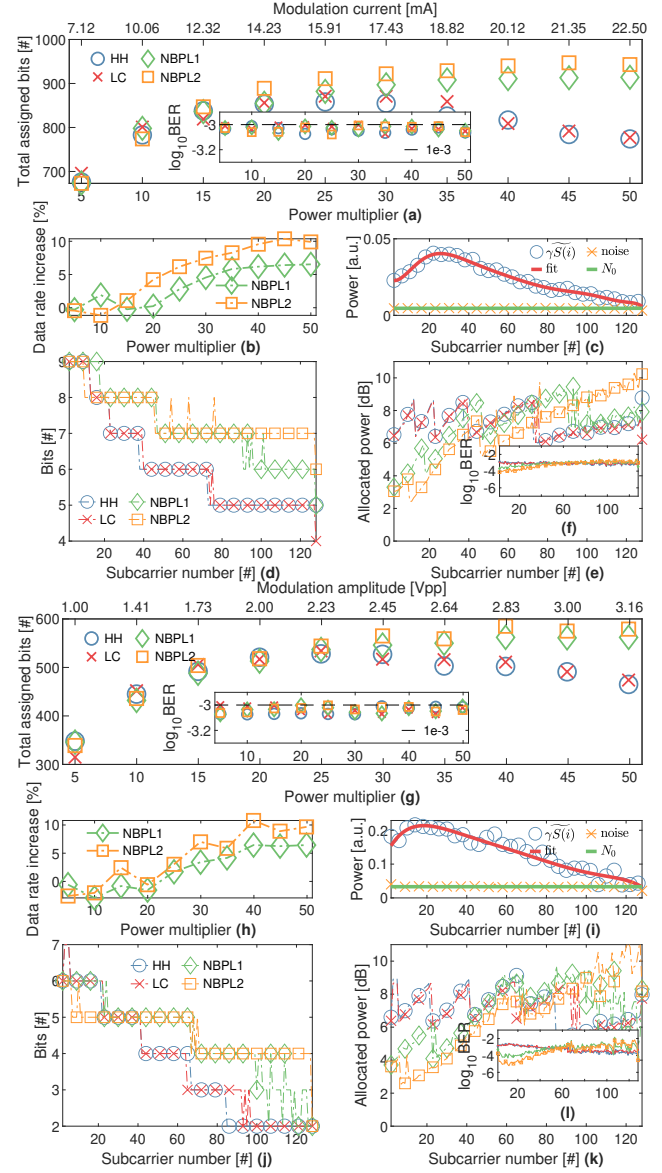20:   **end for**
21: **end while**

Fig. 3. (a) - (f) simulation, (g)-(l) experiment. (a,g) the number of assigned bits, (b,h) throughput increase, (c,i) nonlinear distortion of the OWC channel versus the power multiplier. Note that $\widetilde{\gamma S(i)}$ is the $\gamma S(i)$ multiplied by $(M^2 - 1)(\sum G^2(i)P(i))^2$. (d,j) assigned bits, (e,k) allocated power, and (f,l) estimated BER for each subcarrier at $M = 50$.

(Fig. 2 (d)), thereby confirming its convergence. Second, the transmission capacity for power loading optimized with Algorithm 1 is compared with uniform power loading (Fig. 2 (a)). The capacity in a linear channel, shown with a dotted line, sets the upper bound of achievable capacity. At low input powers, all the capacities are nearly identical, as the ND is small. With increasing power, in a nonlinear LED, the capacity with uniform loading reaches a maximum and starts declining as the ND power increases faster than the input signal power. Notably, the optimized power loading algorithm allows for improvement with respect to the uniform loading capacity by up to 10% (Fig. 2(c)). It is observed that the power distribution obtained using Algorithm 1 varies depending on the maximum power limit, with an almost uniform distribution being the preferred option at low powers, and suppressed power in the low-frequency subcarriers for higher powers, as these subcarriers generate more ND (Fig. 2(b)).

In the following, we evaluate the proposed algorithms in MATLAB simulations. The rate equation LED model [16] is utilized to simulate the LED, with the following parameters: $A=7.85 \times 10^7\,\text{s}^{-1}$, $B=2.38 \times 10^{-8}\,\text{cm}^3\,\text{s}^{-1}$, $C=0\,\text{cm}^6\,\text{s}^{-1}$, $A_w t_w=4.1 \times 10^{-7}\,\text{cm}^3$, $p_0=1.8 \times 10^{15}\,\text{cm}^{-3}$, $n_{DC}=1.45 \times 10^{15}\,\text{cm}^{-3}$, with a bias current of 15 mA. OFDM transmission is simulated using four different BPL algorithms: HH, LC, Nonlinear BPL1 (NBPL1), and Nonlinear BPL2 (NBPL2). In the simulation, we used an OFDM signal with $N=128$ subcarriers, and the highest subcarrier frequency was set to 200 MHz. Algorithms were compared at the same target bit error rate (i.e., 10^{-3}). The performance was assessed from the linear power range (M=1, $I_{mod}=3.19\,\text{mA}$) up to the highly nonlinear operating point (M=50, 22.50 mA). The $\gamma S(i)$ was

calculated from (5), where $\sigma^{(1)}$ and $\sigma^{(M)}$ were estimated at the receiver from the error vector magnitudes (EVM) of QAM-4 loaded training sequences at low (M=1) and high (M=50) input powers, respectively (result in Fig. 3(c)), and a polynomial fit to (5) serves as $S(n)$. The frequency response was estimated using the same training sequence as $G(i) = \frac{Y(i)}{X(i)}$, where Y and X are the received and sent symbols, respectively. The results for nonlinear BPL are shown in Fig. 3. The data rate increase (Fig. 3(b)) is shown with respect to the HH algorithm up to the power where the HH algorithm assigns the maximum number of bits, and with respect to that number for higher powers. At low input powers, where the ND is negligible, all the algorithms' performance is approximately identical. However, for higher input powers, a distinct increase in the number of bits assigned to a symbol is visible for the nonlinear loading algorithms. In conclusion, by using nonlinear BPL algorithms

the maximum transmission rate (as a function of power) can be increased by up to 8% and 10% for NBPL1 and NBPL2, respectively, which is consistent with the theoretical prediction (Fig. 2). NBPL1 was found to be worse than NBPL2. We believe this is caused by the calculation of the predicted remaining capacity, which is done as if the channel was linear. The distribution of the assigned bits and powers (Fig. 3(d)) indicates that the nonlinear algorithms favor loading bits (and power (e)) to higher subcarriers. However, it appears that simple preemphasis plus uniform bit loading is not an optimal solution. The validity of the simplified ND model is confirmed by the BER distribution in the subcarriers, which is practically equal (Fig. 3(f)).

IV. EXPERIMENTAL SETUP AND RESULTS

The experimental setup is presented in Fig. 1(b). In the experiment, a Hamamatsu resonant cavity (RC) red LED L10762 with a peak emission wavelength at 660 nm was used. The measured light-current-voltage characteristic of the RC LED is shown in Fig. 1(c). The diode was biased at 15 mA, and the modulating voltages ranged from 0.45 Vpp to 3.16 Vpp (directly after the amplifier). The signal generated in MATLAB was converted to the analog domain using an arbitrary waveform generator (AWG) and then fed to the LED through a Bias-T. At the receiver, an avalanche photodetector (APD) and an oscilloscope converted the signal to the electrical and digital domains, respectively. The received data was subsequently processed offline in MATLAB. The performance assessment of the four algorithms was carried out across the linear power range (M=1, 0.45 Vpp) up to the highly nonlinear operating point (M=50, 3.16 Vpp). The relationship between the input power and the number of assigned bits per symbol, the data rate increase, and the estimated ND of the setup are shown in Fig. 3(g), (h), (i), respectively, while the power and bit assignment together with the BER versus the subcarrier number are presented in Fig. 3(j), (k), (l). As the highest subcarrier frequency was 200 MHz, nonlinear loading increased the data rate from 776 Mbit/s (HH, M=25, 2.23 Vpp) to 860 Mbit/s (NBPL2, M=40, 2.83 Vpp). Although the simulations were not designed to mimic the experimental setup, the experimental results closely follow the trends from simulations with similar gains for nonlinear BPL1 and BPL2, albeit a slightly greater discrepancy from the LED ND model described in the Introduction is observed. This is seen in the greater fluctuation of the estimated $\gamma S(i)$ curve, as well as the slightly uneven BER across different subcarriers (f), and can be explained by the imperfect heuristic model of ND generation and also possible nonlinearity of other electrical components of the transmission system. The performance of the nonlinear BPL1 and BPL2 algorithms may appear to be somewhat diminished for smaller power multipliers; however, we believe that this can be attributed to random fluctuations in the number of bits assigned due to the relatively high noise in this range.

V. CONCLUSION

In this letter, we have shown for the first time that nonlinearity-aware BPL algorithms in multicarrier commu-

nications over VLC channels can achieve a significant (up to 10%) advantage over classical BPL like HH. Although our analysis is carried out for LED, we believe the principle may be applied to other communications exhibiting frequency dependence of ND, provided that a reliable model for their nonlinearity exists. Although nonlinear equalizers can provide higher gains in throughput, as instead of distributing the signal power to generate less ND, they aim to remove it completely (e.g., a gain of 23.5% in [17]), the nonlinear BPL procedure, once terminated, requires no additional signal processing. The only complication with regard to classical BPL is that they require estimation of the channel in two regimes: at low and high (target) input powers, to estimate the noise power, and nonlinear distortion distribution, respectively. We believe that nonlinear BPL algorithms may now be added to the catalogue of available nonlinearity mitigation methods in multicarrier systems.

REFERENCES

[1] L. Matheus *et al.*, "Visible Light Communication: Concepts, Applications and Challenges," *IEEE Commun. Surveys Tuts.*, vol. 21, no. 4, pp. 3204–3237, 4th Quart. 2019.

[2] M. A. Arfaoui *et al.*, "Physical Layer Security for Visible Light Communication Systems: A Survey," *IEEE Commun. Surveys Tuts.*, vol. 22, no. 3, pp. 1887–1908, 3rd Quart. 2020.

[3] Y. Tanaka *et al.*, "Indoor visible communication utilizing plural white LEDs as lighting," in *Proc. 12th IEEE Int. Symp. PIMRC*, San Diego, CA, USA, Oct. 2001, p. 81–85.

[4] S. Mardanikorani *et al.*, "Sub-carrier loading strategies for DCO-OFDM LED communication," *IEEE Trans. Commun.*, vol. 68, no. 2, pp. 1101–1117, Feb. 2019.

[5] N. Papandreou and T. Antonakopoulos, "Bit and power allocation in constrained multicarrier systems: The single-user case," *EURASIP J. Adv. Signal Process.*, vol. 2008, no. 1, pp. 1–14, Dec. 2007.

[6] J. A. Bingham, "Multicarrier modulation for data transmission: An idea whose time has come," *IEEE Commun. Mag*, vol. 28, no. 5, pp. 5–14, May 1990.

[7] H. Levin, "A complete and optimal data allocation method for practical discrete multitone systems," in *Proc. IEEE Glob. Telecommun. Conf.*, 2001, pp. 369–374.

[8] H. Elgala *et al.*, "A study of LED nonlinearity effects on optical wireless transmission using OFDM," in *Proc. 6th IEEE/IFIP Int. Conf. on Wireless and Opt. Commun. Netw.*, Cairo, Egypt, 2009, p. 388–392.

[9] X. Xu *et al.*, "Power allocation scheme using particle swarm optimization for visible light communication systems," *Optical Engineering*, vol. 62, no. 6, p. 068102, 2023.

[10] L. C. S. Teles *et al.*, "Power allocation methods for OFDM systems with nonlinear power amplifier," in *Proc. IEEE Symp. Comput. Commun. (ISCC)*, Natal, Brazil, 2018, pp. 1002–1006.

[11] M. Baghani *et al.*, "Optimum power allocation in OFDM systems under power amplifier nonlinearity," *Analog Integr. Circuits Signal Process*, vol. 99, no. 1, pp. 33–38, Apr. 2019.

[12] G. Stepniak, "LED communications with linear complexity compensation of dynamic nonlinear distortion," *Applied Optics*, vol. 61, no. 31, pp. 9271–9278, 2022.

[13] G. Stepniak and J. Siuzdak, "Influence of lighting led design parameters on the dynamic nonlinear response," *J. Lightw. Technol.*, vol. 40, no. 4, pp. 954–960, 2022.

[14] T. Kamalakis *et al.*, "Empirical volterra-series modeling of commercial light-emitting diodes," *J. Lightw. Technol.*, vol. 29, no. 14, pp. 2146–2155, Jul. 2011.

[15] S. Boyd *et al.*, "Measuring Volterra kernels," *IEEE Trans. Circuits Syst.*, vol. 30, no. 8, pp. 571–577, Aug. 1983.

[16] X. Deng *et al.*, "Mitigating LED Nonlinearity to Enhance Visible Light Communications," *IEEE Trans. Commun.*, vol. 66, no. 11, pp. 5593–5607, Nov. 2018.

[17] D. Sun *et al.*, "6 Gbps Micro-LED Transmission Using OFDM With Predistortion and Single-Tap Nonlinearity Compensation," *IEEE Photon. Technol. Lett*, vol. 35, no. 14, pp. 781–784, May 2023.